Chem Soc Rev

Photo-responsive Pseudorotaxanes and Assemblies

Journal:	*Chemical Society Reviews*
Manuscript ID:	CS-TRV-09-2014-000295.R1
Article Type:	Tutorial Review
Date Submitted by the Author:	03-Nov-2014
Complete List of Authors:	Das, Amitava; National Chemical Laboratory, Organic Chemistry Division Mandal, Amal; University of Twente, Molecular Nanofabrication Gangopadhyay, Monalisa; National Chemical Laboratory, Organic Chemistry Division

Chem. Soc. Rev.

RSCPublishing

TUTORIAL REVIEW

Photo-responsive Pseudorotaxanes and Assemblies

Cite this: DOI: 10.1039/x0xx00000x

Amal Kumar Mandal[a], Monalisa Gangopadhyay[b] and Amitava Das*[b].

Received ooth January 2012,
Accepted ooth January 2012

DOI: 10.1039/x0xx00000x

www.rsc.org/

Chemists have achieved a predictable control over various non-covalent interactions and have used these weak interactions in their favour for developing a plethora of intricate functional structures. In this tutorial review we have summarized reports on such supramolecular structures that describe the rational approach in designing host and/or guest components, tagged with appropriate fluorophore, for achieving the modified optical responses on formation of an assembly. This has relevance for designing new photo-responsive smart or adaptive stimuli responsive functional materials, self-healable materials, with interesting photo-physical property. These are also important in the area of supramolecular chemistry and biophysical chemistry in predicting relative conformation in solution.

1. Introduction

Supramolecular chemistry has fascinated chemists as well as researchers from the interdisciplinary research areas owing to the possibilities for achieving thermodynamically stable elegant and exotic architectures or assemblies by utilizing various non-covalent interactions.[1-4] Thermodynamic stabilities of such assemblies are often aided and abetted primarily by certain non-bonding interactions like [C-H…O]/[C-H…$N_{[NHR_1R_2]^+}$] and [C-H…π]/ [π-π].[5-8] More recently an increasing number of research articles from different research groups have described that optical response(s), primarily in form of fluorescence, could be used for probing the conformational change(s) of the host and/or guest components that is/are associated with such assembly formation. In general, fluorescence responses are sensitive to immediate environment, which changes drastically upon conformational change under appropriate circumstances. Fluorescence as a technique also offers the possibility in achieving high signal-to-noise ratio even for a dilute solution of the sample. Most importantly, time scale for luminescence process(es) for most organic fluorophores is restricted within the nanosecond time domain, which is generally much faster relative to the time scales for the conformational transitions. Despite several advantages, use of this technique compared to other commonly used techniques (^{1}H-NMR spectroscopy and single crystal X-ray crystallography) for predicting change(s) in molecular conformation, was rather limited till recent past. Recent reports reveal that this could be used as a complimentary technique along with conventionally used methodology like ^{1}H-NMR spectroscopy for understanding any change(s) in molecular conformation/relative orientation or pathways of conformational changes of the host and/or guest molecules on an assembly formation in solution state. In this review article, we have summarized such reports that describe the use of tailored made host and guest molecules for achieveing the desired spectral responses, along with ^{1}H-NMR and X-ray structural data for probing conformational changes on an assembly formation. We have discussed how designing of such host or guest molecules could play a crucial role in inducing the desired photo-induced process(es) that is/are associated with change in molecular conformation. The scope of our discussions are only limited to those literature reports that help in developing an insight to link the structural requirements for the host/guest molecule and optical response that is triggered by various photo-induced processes like photo-induced electron/energy transfer (PET/PeT), photo-induced charge transfer (PCT), Förster Resonance Energy Transfer (FRET) or a sequential process like PET coupled FRET. Intricacies in the design aspect in using the π-π stack interaction for stabilizing such supramolecular architecture as well as the FRET based fluorescence responses are also discussed.

To focus on such a theme we have primarily chosen pseudorotaxane substructure due to its some unique structural features.[9,10] In general, a pseudorotaxane is consisted of two parts, one or more macroring(s) as the host component and a molecular thread as the guest component. A pseudorotaxane complex could be formed reversibly with desired and predicted thermodynamic control by simple mixing of the individual molecular components in solution under the influence of an external stimulus and could also undergo a disassembly process in presence of appropriate counter stimulation, like media polarity, pH, redox potential, solution temperature, etc. Based

on the relative interactions between the host and guest components, different prevalent equilibrium processes that are generally involved in a pseudorotaxane formation are shown in Figure 1.

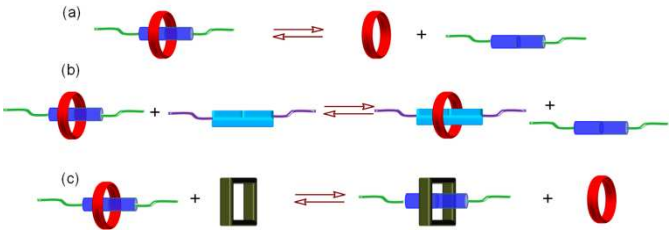

Figure 1. (a) The complexation/decomplexation of a pseudorotaxane, (b) the interchange of a macrocycle between two axel units, (c) interchange of a axel unit between two macrocycles [Adopted from a article by J.F. Stoddart and his co-workers in Angew. Chem. Int. Ed. 2000, 39, 3348].

2. Ammonium ion as a binding motif

2.1 Probable binding mode.

In his seminal paper, Pedersen reported that dibenzo-[l8]-crown-6 (DB18C6) formed 1:1 complexes with primary alkyl ammonium ions (RNH_3^+) and failed to do so with secondary dialkyl- ($R_2NH_2^+$) as well as tertiary trialkyl- (R_3NH^+) ammonium ions for steric constrain.[11,12] Generally, RNH_3^+ could adopt two different orientations (*perched* and *nested*) with respect to the DB18C6 in their corresponding host-guest complex depending upon the relative orientations of the [N-H…..O] hydrogen bonding interactions (Figure 2). Among these two orientations, "*perched*" geometry is generally more common. Trueblood proposed that the primary factor that governed the geometry in such host-guest adduct was the depth of penetration of the $-NH_3^+$ group.[13] Previous studies proposed that secondary dialkylammonium ($R_2NH_2^+$) ions would prefer to form host-guest complex with crown ethers in such a way as to place the $-NH_2^+$ centre within the plane of the macrocyclic ring. This proposition was first experimentally demonstrated by Stoddart et al..[14,15] They could demonstrate that secondary dialkylammonium ions formed host-guest adducts with macrocyclic polyethers, such as DB24C8. Such adduct formation was stabilized predominantly by hydrogen bonding interactions involving $H_{R_2NH_2^+}$ and $O_{\text{Crown ether}}$ moiety.

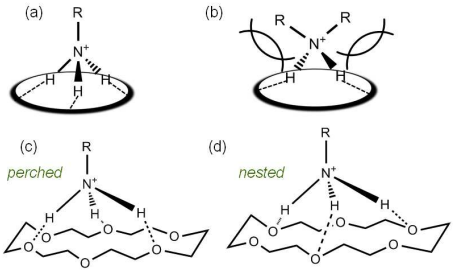

Figure 2. Cartoon representations of (a) the three-point binding of a primary alkylammonium ion (RNH_3^+) and (b) the two-point binding of a secondary dialkylammonium ion ($R_2NH_2^+$) with DB18C6 and the corresponding (c) "*perched*" and (d) the "*nested*" geometries found in the solid state [Adopted from a article by J.F. Stoddart and his co-workers in Chem. Eur. J. 1996, 2, 709].

2.2 Conformational motion in ammonium based pseudorotaxane

Various non-covalent interactions like hydrogen bonding and π-π stack interactions generally prevail in the formation of an inclusion complex and consequently induce a change in molecular conformation or movement in the participating molecules. These reversible molecular movements provide the basis for the construction of artificial molecular machine. Such molecules are generally consist of three parts i.e.; an active site, a remote site and a photoactive unit which transmit binding induced information from one site to other. In certain cases these two sites (active and remote sites) are connected by a photoactive unit which is capable of producing two conformational isomers upon excitation with light of a specific wavelength. Among these two conformations, the folded one favours the electrostatic attraction and thus, the H-bonded adduct formation between $-NH_3^+$ and the crown ether moiety.

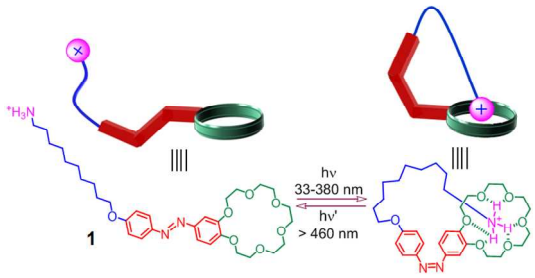

Figure 3. The photoinduced *cis/trans* isomerisation of azobenzene unit of **1**, is accompanied by the motion of its cationic tail which only interact with macrocyclic head in the *cis*-form.

Shinkai et. al. had demonstrated this principle at molecular level using compound **1**, where the active sites (ammonium unit) and the remote site (crown unit) were linked through a photoactive azobenzene unit (Figure 3).[16] Photo-isomerization of the azobenzene unit upon excitation within a wavelength range of 330-380 nm, led to the generation of *cis*-isomer that brings $-NH_3^+$ and the crown unit in close proximity to allow an intramolecular association, which altered the affinity of the crown ether fragment towards a metal ion. Such a phenomenon was not possible for the corresponding *trans*-form and the crown ether fragment of this *trans*-form showed higher affinity towards metal ions. This was one of the early reports that described the significance of conformational changes for an appropriate host-guest interaction.

Recently, we have reported a host-guest approach for imposing a structural confinement on a triphenylamine (TPA) derivative for suppressing the non-radiative relaxation processes associated with its conformational motion.[17] Three different host molecules, namely CB[7], β-CD and DB24C8, were used for studying inclusion complex formation with a secondary ammonium salt of a TPA derivative as the guest molecule (Figure 4). Such host molecules were chosen based on their comparable cavity volume but different geometrical features and cavity surface potential. The extent of complexation and topography of the inclusion processes during complexation with three different host molecules have been established

through MALDI-TOF Mass, ^{1}H-NMR and 2D-NOESY experimental studies. ^{1}H-NMR studies also revealed the cooperative binding process for CB[7]; while statistical binding prevailed for hosts like β-CD and DB24C8.

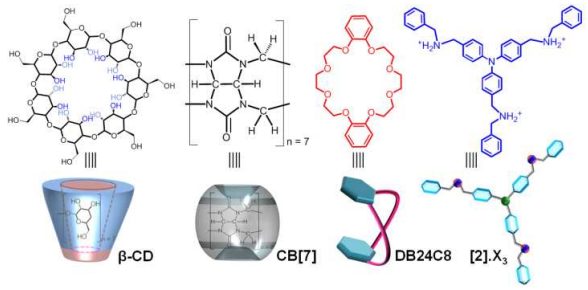

Figure 4. Schematic representation of different macrocyclic hosts and the guest molecules used to study the conformational restriction through complexation.

TPA derivative $\mathbf{2}^{3+}$ showed solvatochromic behaviour with a weak emission (Φ^2 = 0.0099) in the free state. However, an appreciable increase in quantum yields ($\Phi^{2.\{CB[7]\}3}$ = 0.0283 and $\Phi^{2.\{\beta\text{-}CD\}3}$ = 0.0182) and average lifetimes of the photoexcited states were observed on complexation with CB[7] or β-CD and these were attributed primarily to the restricted rotational freedom of the TPA-based core in $[\mathbf{2}\bullet\{\beta\text{-CD}\}_3]^{3+}$ and $\mathbf{2}\bullet\{CB[7]\}_3$ (Figure 5). Reduction of local polarity around the TPA-core within the macrocyclic cavity might have also contributed to this. ^{1}H-NMR studies revealed an incomplete complex formation between DB24C8 and $\mathbf{2}(PF_6^-)_3$ during [4]pseudorotaxane formation.

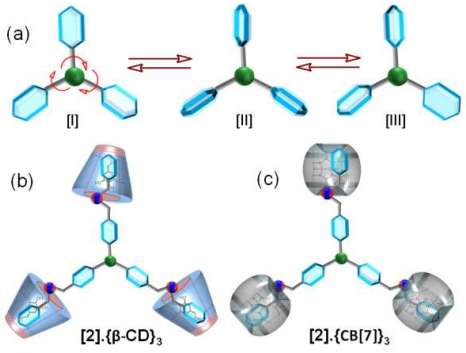

Figure 5. (a) Conformational change of a TPA core through internal bond rotation. (b), (c) Mode of complexation of $\mathbf{2}.Cl_3$ with β-CD and CB[7].

However, luminescence spectral responses for formation of $[\mathbf{2}\bullet\{DB24C8\}_3]^{3+}$ were more interesting. On excitation of DB24C8 fragment at 280 nm, a FRET based energy transfer from DB24C8 moiety in $[\mathbf{2}\bullet\{DB24C8\}_3]^{3+}$ to the TPA core was observed along with a subsequent increase in emission quantum yield for the TPA core at 369 nm (Figure 6). Thermodynamic feasibility for the FRET process, involving the low lying excited state of DB24C8 as the donor state and the even lower lying excited state of $\mathbf{2}^{3+}$ as the acceptor state, supported such a presumption. The restricted internal rotation of the TPA core on formation of $[\mathbf{2}\bullet\{DB24C8\}_3]^{3+}$ could have also contributed to this observed enhanced TPA based emission. Apparently, there was an apparent disagreement between the energy transfer efficiency values, calculated on the basis of quantum yield (71%) and the time resolved spectral data (28%). Trivial sensitization effect, in addition to the FRET based process, was operational between the free components and could be accounted for this apparent disagreement.

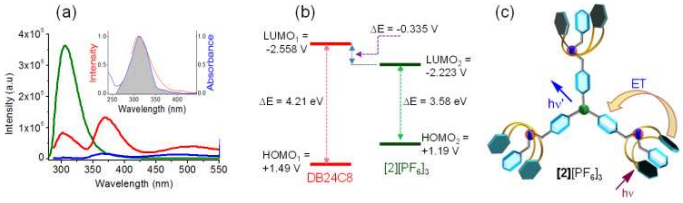

Figure 6. Emission spectra for (a) DB24C8 [2.2 x 10^{-5} M, green line], $\mathbf{2}(PF_6^-)_3$ in presence 3 mole equiv. of DB24C8 (red line), and $\mathbf{2}(PF_6^-)_3$ (7.3 x 10^{-6} M, blue line) using λ_{ext}: 280 nm; Inset: Emission and absorption spectral overlap for DB24C8 and $\mathbf{2}(PF_6^-)_3$, respectively. (b) Relative energies for the HOMO and LUMO levels for DB24C8 and $2(PF_6^-)_3$; (c) Schematic representation of the mode of complexation of DB24C8 with $\mathbf{2}(PF_6^-)_3$. [Figure is reproduced from Ref 17]

2.3 Coupled photo-physical response in ammonium based pseudorotaxane

A coupled photo-physical response always have some practical advantage for studying the conformational dynamics as it allows simultaneous detection of two signals resulting from two states of the sample. This helps in overcoming the practical limitation imposed for quantitative measurement by using single detection window. Balzani et al. were the first to demonstrate such concepts in the hydrogen bonded host-guest adducts to develop the molecular level *plug-socket* system (Figure 7).[18] Guest molecule **3** with anthracene as the fluorescent label gave a *fluorescence turn-ON* response in presence of acid due to an interruption of the PET process. The design of the host and guest molecules allowed them to achieve a spectral overlap between the donor (DB24C8) emission and acceptor (anthracene) absorption spectra. This initiated a coupled *turn-ON* FRET response on [2]pseudorotaxane formation in presence of acid (Figure 7a).

In a subsequent publication they extended this concept by using another photoactive crown ether derivative **4** having binapthyl moiety as the fluorescent label (Figure 7b).[19] The unique choice of the anthracene and binapthyl derivatives helped in achieving the FRET process between the donor binapthyl moiety and acceptor anthracene moieties. In presence of stoichiometric amount of acid, protonated amine moiety ($\mathbf{3}H^+$ or $\mathbf{5}H^+$) eventually formed [2]pseudorotaxanes ($\mathbf{4}\bullet\mathbf{3}H^+$ or $\mathbf{4}\bullet\mathbf{5}H^+$) with **4**. Protonation of the N_{Amine} in **3** or **5**, initiated an interrupted PET process and an associated *turn-ON* fluorescence response from the anthracene core. This further induced a FRET response in $\mathbf{4}\bullet\mathbf{3}H^+$ or $\mathbf{4}\bullet\mathbf{5}H^+$ (Figure 7b). Reversible nature of the pseudorotaxane formation was established in presence of acid or base, respectively. This FRET responses also confirmed a conformation in the respective [2]pseudorotaxane that favoured the proximity of the donor binapthyl and the acceptor anthracene moieties in $\mathbf{4}\bullet\mathbf{3}H^+$ or $\mathbf{4}\bullet\mathbf{5}H^+$. A conformational change for favouring the π-stacking interaction was also

proposed based on the results of ^{1}H-NMR and DFT studies. Fluorescence titration with λ_{Ext} of 292 nm and λ_{Ems} of 360 nm in CH_2Cl_2 medium helped in evaluating an association constant of the order of 10^5 (mol^{-1}) × L for the adduct **4•3**H^+ or **4•5**H^+. However, error associated with the unquenched fluorescence that may arise from binapthyl moiety of the uncomplexed crown ether derivatives was not corrected for the absorption of the acceptor anthracenyl moiety. The energy transfer rate constant was estimated to be ~10^9 s^{-1}.

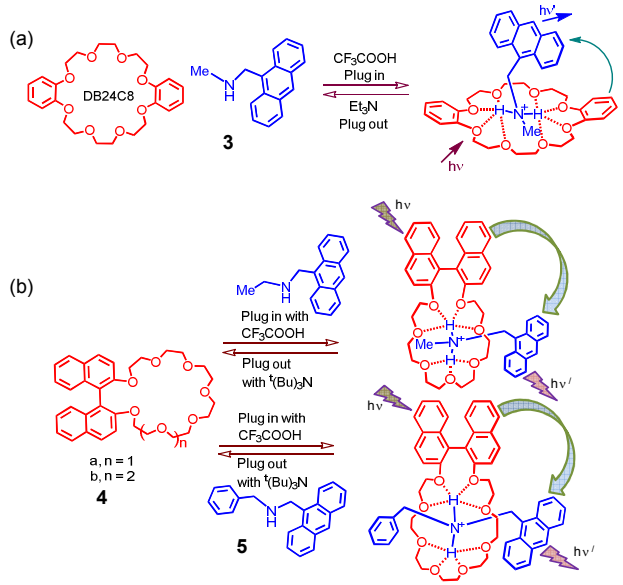

Figure 7. Schematic diagram to demonstrate molecular level *plug/socket* behaviour in an acid/base driven complexation process in hydrogen bonded pseudorotaxanes using (a) DB24C8 and (b) **4** as host molecules.

More recently, we extended such a concept to achieve a more complex system, where one could have additional control on the input signal and the consequential modified output response.[20] To demonstrate such a process, we utilized a supramolecular assembly where the threading phenomena resulted an interrupted PET and *fluorescence on* response, which in turn initiated a FRET process. An azacrown moiety was used as a host **6** and was separated from the photoactive pyrene unit by -CH_2- spacer (Figure 8). The unshared pair of electrons of the tertiary N_{Crown} participated in an efficient PET process and thereby accounted for the observed quenched luminescence of the pyrene unit in **6**. Further, appropriate choice of the donor (pyrene) and acceptor (anthracene) moieties in the respective host and guest units with significant spectral overlap allowed a FRET-based response. Four different guest molecules with varying the stopper size were used for studies. Results of the ^{1}H-NMR and isothermal calorimetric studies (ITC) revealed that guest molecules **7**, **8** and **9** with relatively less steric constrain could form threaded complexes with **6**, while guest molecule **10**, with bulky stopper unit, failed to do so. The association constant for adducts **6•7** ((8.1 ± 1.7) x 10^3 M^{-1}), **6•8** ((4.47 ± 1.0) x 10^3 M^{-1}) and **6•9** ((1.45 ± 0.4) x 10^4 M^{-1}) were evaluated from the ITC measurements, which showed a systematic increase in values on changing the stopper size in the guest molecules. Thermodynamic data also indicated that adducts were stabilised through H-bonding interactions, in addition to π-π stacking interaction. ^{1}H-NMR studies also confirmed distinct π-π stacking interaction between the pyrene and anthracene moieties in all three complexes **6•7**, **6•8** and **6•9**. However, emission responses due to the interrupted PET process involving the lone pairs of electron of the N_{Crown} was complicated on successive increase in [**7**]/[**8**]/[**9**] while titrating with **6**. Such observation was rationalized based on the results of the density functional theory (DFT) calculations as well as results of the molecular dynamic simulations studies. Such studies revealed that there was a possibility of proton transfer from the guest unit **7**/**8**/**9** to the host **6** during complexation process and such a possibility was affected by the relative proton affinities of the different guest molecule as compared to the amine functionality of the host molecule **6**. The calculated results also revealed that for the inter-woven complex **6•7**, *head-to-head* stacking interaction between anthracene and pyrene was energetically preferred than that for the *head-to-tail* orientation by 12.5 kJ/mole in CH_2Cl_2 medium. Such interaction was also evident in the results of the ^{1}H-NMR studies. In addition, such a conformation with *head-to-head* stacking orientation between the anthracene moiety with respect to pyrene moiety could possibly be better suited for the transfer of a H^+ from the $\{\text{-(H)NHR}^+\}_{guest}$ to $\{\text{-(N)H}_2\}_{host}$ and eventually resulted in a more efficient FRET process.

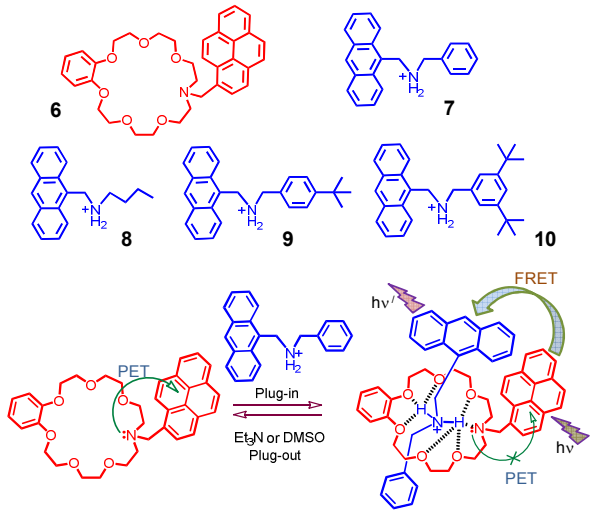

Figure 8. The structures of the azacrown based host and the hexafluorophosphate salt of different guest molecules with varying stopper size and the schematic representation of their stimuli dependent complexation and decomplexation process with associated photo-induced processes.

Liu et. al. demonstrated that the change in an external stimulus such as pH could be a simple and accessible strategy for modulating the coupled photo-physical responses in the multicomponent supramolecular assemblies (Figure 9).[21] They had utilized the affinity of acridine red **AR** to form an inclusion complex **11.**H^+•AR in aqueous solution with β-CD tagged with protonated triarylamine moiety (**11.**H^+). The fluorescence intensity of **AR** was significantly enhanced upon stepwise addition of **11** in the neutral solution due to the formation of

adduct **11**•AR. On excitation at 335 nm (λ_{Max}^{Abs} for **11**), an emission band with λ_{Max}^{Ems} appeared at 363 nm. This emission band maximum shifted to 440 nm in presence of H^+ due to formation of **11H**$^+$ and this favoured the ICT process between phenoxy (donor) and protonated pyridyl moieties (acceptor). Spectral overlap that was achieved between this $ICT_{Emission}$ and absorption band of **AR** in **11H**$^+$•**AR**, initiated a FRET process from the excited **11**H$^+$ as donor to the included **AR** dye as acceptor with an energy transfer efficiency of ~28%. Fluorescence titrations enabled authors to evaluate respective association constants for **11•AR** and **11H**$^+$•**AR** as 8.39 x 10^3 M^{-1} and 2.29 x 10^4 M^{-1}. Reversibility of the binding process as well as the optical responses was established on addition of OH^- to a solution of **11H**$^+$•**AR**.

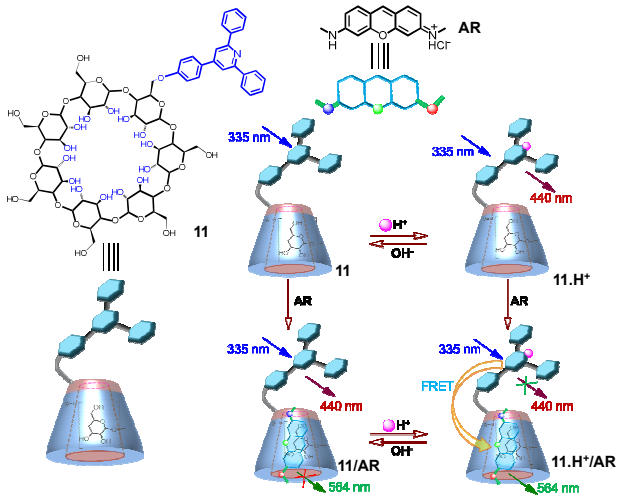

Figure 9. The chemical structures of the host and guest components and the schematic illustration of the switching process as a function of media pH.

2.4 Pseudorotaxane based lanthanide switch

Liu and co-workers also reported luminescent lanthanide switch through controlled photo-physical response of pseudorotaxane in the presence of external stimuli such as K^+ or 18-crown-6 (18C6). Initially a DB24C8-based host molecule **12** with an appended PDCA (pyridine-2,6-dicarboxylic acid) moiety was used for the synthesis of the corresponding 3:1 coordination complex $[(\mathbf{12})_3Tb]^{3+}$ (Figure 10).[22] Host molecule **12** served the purpose of chelator as well as the sensitizer for the Tb^{3+} and accounted for the characteristic Tb^{3+}-based luminescence of $[(\mathbf{12})_3Tb]^{3+}$ with λ_{Ext} of 283 nm. A secondary ammonium ion **13**(PF_6^-), functionalized with a ferrocenyl (Fc) moiety, formed a [4]pseudorotaxane like structure $[(\mathbf{12})_3Tb]\bullet[\mathbf{13}(PF_6^-)]_3$, where the luminescence of the lanthanide core was significantly quenched due to an effective PET process between photoexcited **12** and Fc moieties. Studies with model systems revealed that the formation constant for **12•13**(PF_6^-) (K_a = 1.2 x $10^3 M^{-1}$) was lower than that for DB24C8 and K^+ (K_a = 7.8 x 10^3 M^{-1}) and thus, K^+ could displace **13**(PF_6^-) from the [2]pseudorotaxane complex **12•13**(PF_6^-). This preference of the DB24C8 moiety towards K^+ was utilized for generation of

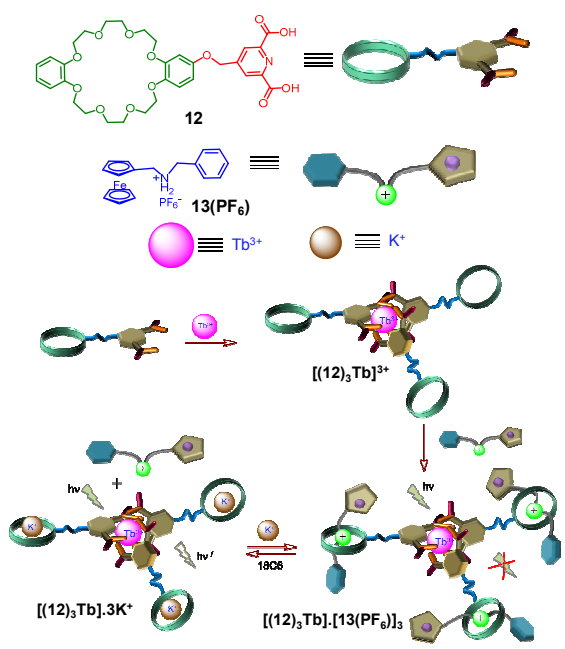

Figure 10. Schematic representations of the coordination mode for $[(\mathbf{12})_3Tb]\bullet[\mathbf{13}(PF_6^-)]_3$ and reversible complexation in presence of K^+ and 18C6.

luminescent $[(K\mathbf{12})_3Tb]$ from the non-luminescent $[(\mathbf{12})_3Tb]\bullet[\mathbf{13}(PF_6^-)]_3$. Much higher affinity of K^+ towards 18C6 (K_a = 1.3 x 10^6 M^{-1}) was used for the regeneration of the non-luminescent $[(\mathbf{12})_3Tb]\bullet[\mathbf{13}(PF_6^-)]_3$ by treating $[(K\mathbf{12})_3Tb]$ with 18C6 in presence of **13**(PF_6^-). Thus, these luminescence responses could be utilized for probing the reversible formation of the [4]pseudorotaxane complex and is shown in Figure 10.

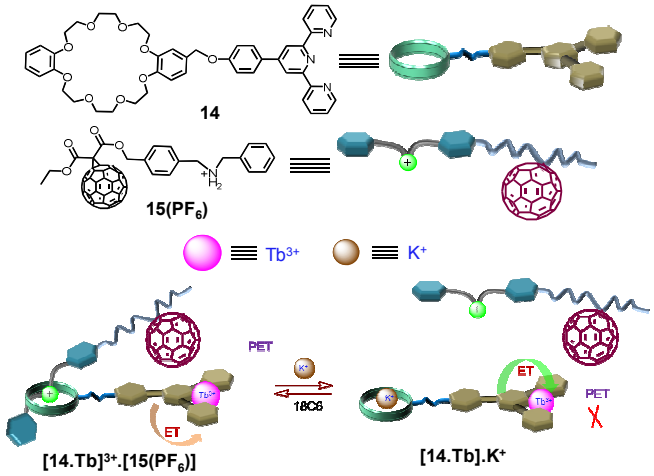

Figure 11. Molecular structures for **14** and **15(PF$_6$)** and schematic representations of the [2]pseudorotaxane (**[14Tb]$^{3+}$•[15(PF_6^-)$_3$]**) with associated luminescence response on reversible complexation and decomplexation process.

They had extended the similar concept for another system having a pendant terpyridyl moiety **14** instead of PDCA (Figure 11).[23] This could form a 1:1 luminescent complex (K^+[**14**Tb^{3+}]; K_a = 1.8 x 10^5 M^{-1}) with Tb^{3+}. As described earlier, PET from **14** caused the sensitization of the Tb^{3+}-core. C_{60} is known to be a good electron sink and thus, [2]pseudorotaxane

([**14**Tb]$^{3+}$•[**15**(PF_6^-)$_3$]) formation induced an efficient quenching of the singlet excited state of Tb^{3+}-based emission. Thermodynamic feasibility of the PET process (ΔG_{PET} = -0.54 eV) was evaluated from the equation 1 and this also favoured such a possibility.

$$\Delta G_{PET} = E_{Ox} - E_{Red} - E_{oo} - (14.4/\varepsilon d) \quad \text{Eq. 1}$$

where, ε was the dielectric constant of the medium (CH_2Cl_2 = 9.1) and d is the distance between C_{60} and terpyridine (7.50 Å; estimated from the optimized structure for [**14**Tb]$^{3+}$•[**15**(PF_6^-)$_3$]).

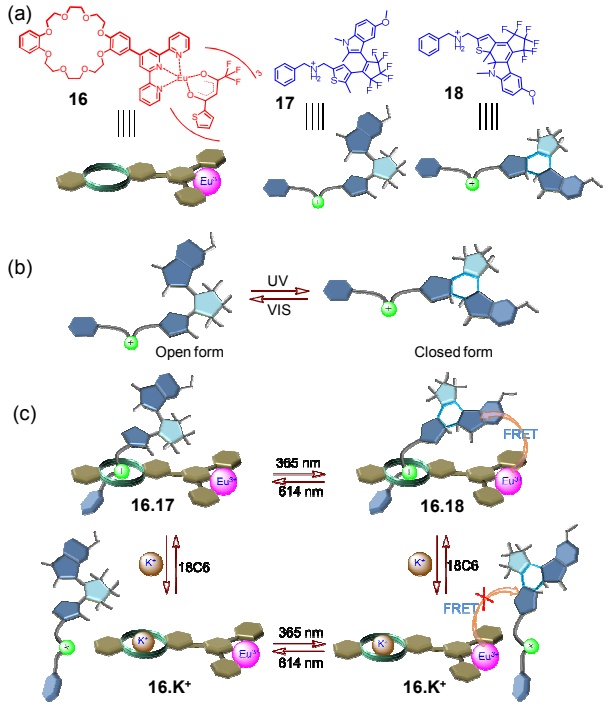

Figure 12. Schematic representations of (a) the compounds that were used for the study, (b) photo-isomerisation of compound DAE in presence of UV and visible light and (c) reversible complex formation and associated optical responses in presence of external stimuli.

The same group also reported another interesting molecular switch using Eu(III)-complexes **16** and a photochromic moiety **17**.[24] Perfluorocyclopentene derivative showed reversible and bistable photochromism between open (**17**; OF) and a closed (**18**; CF) forms (Figures 12a & 12b). OF of the compound (**17**; λ_{Max}^{Abs} ~340 nm) on irradiation with 365 nm light in $CH_3CN/CHCl_3$ medium led to the generation of the CF **18**, having λ_{Max}^{Abs} of 586 nm; while the colourless OF form was restored on irradiation with 614 nm light. ^{1}H NMR studies confirmed the [2]pseudorotaxane formation **16•17** in $CH_3CN/CHCl_3$ medium (Figures 12c). Quantum yields for the photocyclization ($\Phi o_F \rightarrow c_F$) process for the active conformer were determined to be 0.38 for **17** and 0.20 in **16•17**. Steady state and time resolved emission studies revealed the occurrence of the FRET process involving Eu^{3+} as donor (D) and CF form **18** as acceptor (A) in **16•18**. Spectral overlap between D and A as well as the short centre-to-centre distance (20.2 Å) between **18** and Eu^{3+} in **16•18** enabled the FRET process. The choice of the diarylethene derivatives **17** or **18** as the photochromic compound helped also in achieving thermally irreversible photochromic behaviour and outstanding fatigue resistance. Reversibility in the [2]pseudorotaxane formation and associated optical response could be achieved based on the appropriate ionic/molecular inputs like K^+ or 18C6 (Figure 12c). This was a unique example to reveal that a reversible/bistable photochromic compound could be integrated into a supramolecular assembly for generating a FRET based fluorescence response and to demonstrate how stimuli dependent emission responses could be used for probing the assemble formation from individual components.

2.5 Pseudorotaxane based light harvesting system

Photosynthetic light harvesting organisms generally use several chromophores to transfer absorbed solar radiation to a reaction centre in a stepwise and unidirectional manner. In this regard, self-organized assemblies of chromophores could be a better model to understand the transfer of excitation energy in natural system that happens in a diffusive manner at each step with minimum loss in transferred energy. Analysis of FRET-based luminescence response offers the opportunity to retrieve information on molecular proximity, orientation and conformation on the nanometer scale as well as the dynamics of macromolecules and molecular assemblies in solution.

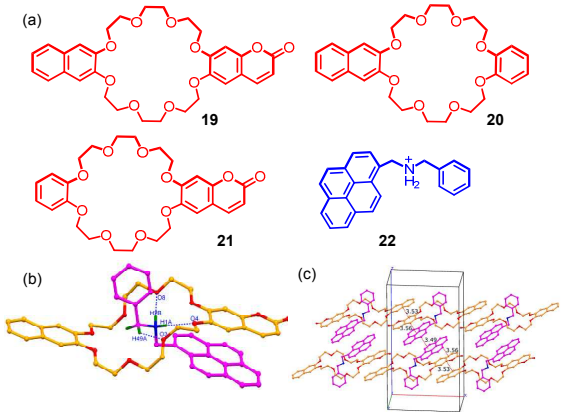

Figure 13. (a) Molecular structures of hosts **19**, **20** & **21** and guest **22** components; (b) Single crystal X-ray structure of the pseudorotaxane assembly. Hydrogen atoms and hexafluorophosphate ions are not shown for clarity; (c) packing diagram depicting the bilayer arrangement of the molecule with the stacking interaction between the aromatic rings. [Figure is adopted from Ref 25]

Recently, a trichromophoric pseudorotaxane, comprised of primary donor (I) – primary acceptor (II) /secondary donor (II) – secondary acceptor (III) pairs, had been used to demonstrate a sequential energy transfer (I→II→III) along with direct energy transfer (I → III) process (Figure 13).[25] The ability of the dibenzo crown ether derivative **19** to form interwoven pseudorotaxane complex with secondary ammonium ion derivative **22** was utilized to demonstrate this phenomenon. For this, naphthalene (I) and coumarin (III) were used as the primary donor and secondary acceptor, respectively; while pyrene (II) unit, having spectral overlap with both I and III, was

used as the primary acceptor as well as the secondary donor. Detailed ^{1}H-NMR studies in solution as well as result of the single crystal X-ray structural study confirmed the complexation process both in solution and in solid state. Crystal structure revealed that in addition to hydrogen bonds, intramolecular π-π stack interaction between the pyrene and coumarin rings (3.56 Å) and C–H/π interaction between the H_{Phenyl} atoms of **22** and the naphthalene ring contributed to the stability of the assembly formation (Figure 13b). The formation constant (K_a = 2.31 x 10^3 M^{-1}), ΔG (-19.25 kJ mol^{-1}), ΔH (-36.45 kJ mol^{-1}), and TΔS (-17.20 kJ mol^{-1}), for the [2]pseudorotaxane were evaluated using ITC titration studies.

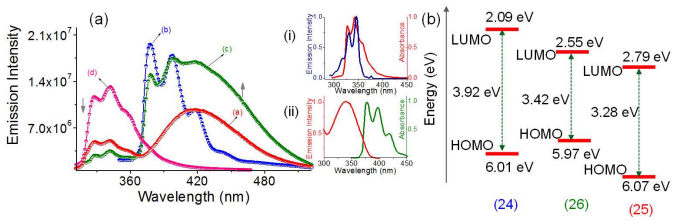

Figure 14. (a) Emission spectra of (a) **19** (λ_{Ext} of 280 nm), o & —; (b) **22** (λ_{Ext} = 310 nm), o & —; (c) 1:1 mixture of **19** & **22** (λ_{Ext} of 280 nm), o & —; and (d) **20** (λ_{Ext} = 280 nm), o & —. Inset: Spectral overlap between (i) luminescence spectrum of **21** and electronic spectrum of **22**; (ii) luminescence spectrum of **22** and electronic spectrum of **21**. (b) Schematic presentation of respective energy levels of donor **20**, transmitter **22** and acceptor **21** [Figure is reproduced from Ref 25].

Steady state and time resolved emission studies revealed that for the sequential energy transfer process (I → II → III) of the triad system **19•22**, pyrene acted as a transmitter and whole supramolecular assembly behaved as a linear energy transferring wire. Sensitized emission of the coumarin moiety, offered the possibility of evaluating the performance of this linear trichromophoric system by one and two-step FRET mechanisms. Fluorescence decay traces (λ_{Ext} = 280 nm) monitored at 470 nm (λ_{Max}^{Ems} for coumarin) for **19** showed a negative pre-exponential factor (time constant of 0.32 ±0.005 ns), which confirmed the energy transfer process between naphthyl and coumarin moieties with an energy transfer efficiency of 96%. These studies also enabled authors in calculating the Förster distance of 26.9 Å between two interacting fluorophores in **19**. Similar studies for **19•22** with λ_{Ext} = 280 nm & λ_{Mon} = 378 (predominantly pyrene based emission) confirmed a Förster energy transfer from naphthalene to pyrene with a time constant of ~11ns. Energy transfer rate between pyrene and coumarin could not be evaluated—presumably due to different overlapping kinetic traces. Analogous studies with model [2]pseudorotaxanes, **20•22** and **21•22**, confirmed a simultaneous FRET process involving I and III (Figure 14). Thermodynamic feasibility of this sequential energy transfer process was confirmed from the evaluation of the relative energy levels of the interacting fluorophores (Figure 14b).

Li and co-workers demonstrated a new strategy for enhancing the energy utilization in light-harvesting dendrimers through a controllable pseudorotaxane formation at the periphery.[26] They synthesised a series of water-soluble dendrimers $[\mathbf{23}]_n(NapH)_x$ having several pendant napthyl moieties. Steady state fluorescence studies revealed that strong interactions among peripheral napthyl moieties in those dendrimers resulted in the formation of several excimers with low fluorescence quantum yield values. Use of CB[7] led to the formation of several pseudorotaxanes, which could best be represented as xCB[7]•$[\mathbf{23}]_n(NapH)_x$ (Figure 15). This pseudorotaxane formation effectively suppressed the energy dissipation through excimer formation and accounted for the significant enhancement in the fluorescence quantum yields for these dendrimers.

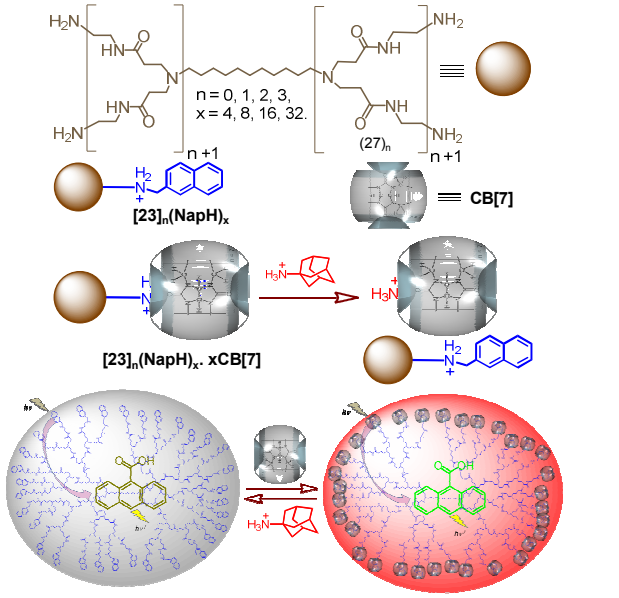

Figure 15. Chemical structure of the dendrimer $[\mathbf{23}]_n(NapH)_x$ and the schematic representation of enhancement of energy utilisation due to pseudorotaxane formation at the periphery. [Figure is partially adopted from Ref 26]

To investigate the harvested energy utilization, 9-anthracenecarboxylic acid (AN) as an acceptor for energy was introduced into these dendritic systems. Typically, the efficiency of energy transfer from periphery of the free dendrimers to the encapsulated AN was poor. However, for xCB[7]•$[\mathbf{23}]_n(NapH)_x$ this was favoured and a much higher emission quantum yield for AN-based fluorescence was observed. This was further confirmed from the fact that the energy transfer efficiency was ~1.5 times higher for 32CB[7]-•$[\mathbf{23}]_3(NapH)_{32}$-AN than 16CB[7]•$[\mathbf{23}]_2(NapH)_{16}$-AN. Higher inclusion affinity of the adamentyl moiety towards CB[7] was nicely utilized for demonstrating the reversibility of above referred inclusion process and the initial fluorescence response of the parent dendrimer $[\mathbf{23}]_n(NapH)_X$ was restored in presence of externally added adamantly amine. Thus, this example demonstrated a noncovalent approach for controlling the undesired chromophore-chromophore interactions and the excited state energy dissipation process.

3. Paraquat derivatives as binding motif

3.1 Probable binding mode

Paraquat derivatives (N,N′-dialkyl-4,4′-bipyridinium salts) have been used as an active site as guest components in supramolecular chemistry for their facile synthesis and high binding ability with different macrocycles.[27-31] Using crown ether-paraquat interactions as a recognition motif, a series of supramolecular systems are fabricated with high efficiency. In such assembly process, two different conformations for crown ether based hosts are generally observed. Either a pseudorotaxane structure (Figure 16), where paraquat unit is threaded through the crown ether or an "exo" or "hot dog" or "taco" complex formation is observed. Preorganization of the crown unit for adopting a folded conformation is essential for the "exo" or "hot dog" or "taco" complex formation (Figure 16). Charge transfer interactions as well as H-bonding and electrostatic interactions were responsible for such intra-complex stabilization.

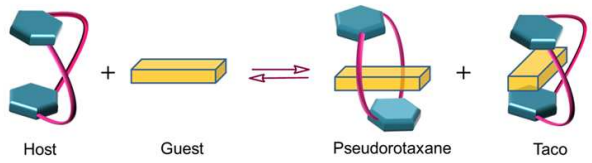

Figure 16. Schematic representation of pseudorotaxane and a taco complex formed between dibenzo crown ether derivative and paraquat ion.

3.2 Structure dependent conformational change

In this section we have discussed how slight structural changes as well as the presence of counter anion of the paraquat derivative could influence the conformational change(s) of the assembly. In an earlier communication from this research group, two different binding modes (i.e. a "taco complex" and a "pseudorotaxane complex") were reported while studying the complexation process between a divalent crown ether **24** and structurally analogous paraquat derivatives $[PQT]^{2+}$ and **25** with different stopper size as guest molecules (Figure 17).[32] Divalent crown ether **24**, having two different photoactive naphthalene derivatives as signalling fragments as well as two DB24C8 derivatives as the receptor fragment was used for studies. Details ^{1}H-NMR studies revealed that preorganized host **24** in its folded conformation formed [3](taco complex) with two parquat units of $[PQT]^{2+}$ and binding of these two $[PQT]^{2+}$ units were cooperative. However, similar studies revealed that the complexation between **24** and the **25**$(PF_6^-)_2$ resulted a [3]pseudorotaxane structure. Results of the steady state and excited state emission as well as electrochemical studies suggested the formation of a new charge transfer (CT) state on "taco" complex formation. The reversible host-guest adduct formation was demonstrated in presence of KPF_6 and DB18C6 (Figure 17b). Three processes, namely assembly, de-assembly and re-assembly, could be probed by distinct changes in luminescence spectral response associated with each of these three processes. These observed fluorescence responses at appropriate monitoring wavelengths could be correlated in principal for demonstrating different logic operations. Fluorescence changes at certain wavelengths were used as output signals for two independent inputs (In1 and In3; In1 and In2) to demonstrate basic logic operations like OR and YES gates, respectively; while an INHIBIT gate could be demonstrated using three inputs (Figure 17c, 17d and 17e). This is one of the rare examples in the contemporary literature where a supramolecular assembly is used to demonstrate complicated Boolean operators like INHIBIT gate.

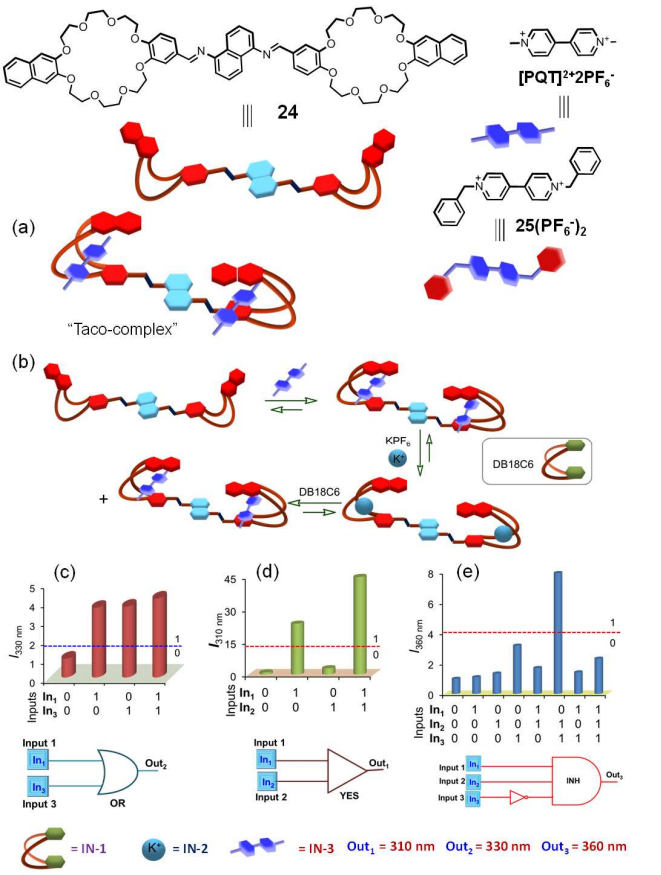

Figure 17. Molecular structure of **24**, $\mathbf{PQT^{2+}}$ and **25**. Schematic representations (a) of the [3](taco complex), (b) reversible complexation process in presence of K^+ or DB18C6. Bar diagrams showing (c) for the OR logic states, (d) for the YES logic states, (e) for the INHIBIT logic states of the system. [Figure is reproduced from Ref 32]

Gibson and co-workers thoroughly examined the possible influence of counter anions on conformational change. They observed a 6.8-fold increase in association constant in presence of ditopic H-bond accepting counter anion **29**-TFA compared to **28**-PF_6^-, while a crown ether based guest molecule (**26**) was used.[33] It was proposed that folding of **26** on formation of the exo- or taco-complex with $\mathbf{27}^{2+}$ was assisted by H-bonding interactions with the ditopic TFA ion with two OH_{-CH_2OH} functionalities of the crown ether derivatives (Figure 18). These led to the formation of a supramolecular cryptand and stabilized the three-component complex. A similar influence was also observed for tridentate OTs^- with 1.5-fold enhancement in association constant as compared to those for the nonchelating PF_6^- and BF_4^-.

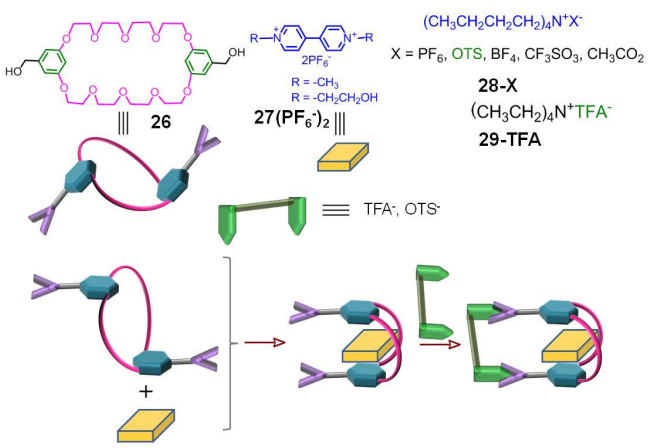

Figure 18. Structure of the host **26** and the cartoon representation of the cooperative Host/Guest Interaction via chelation event.

They also demonstrated that seven species could be self-assembled to form a pseudocryptand-based [3]pseudorotaxane (**30b**)$_2$•**31**-TFA.2H$_2$O on addition of tetraethylammonium trifluoroacetate (TEATFA) to a solution of **30b** and bisparaquat **31**-X (Figure 19a).[34] Crystal structur revealed that, hydroxy group of each host **30b** was connected via a TFA counterion and a water molecule through hydrogen bonding interactions to form a new pseudocryptand and two of these enshrouded the guest in a *face-to-face* orientation (Figure 19b).

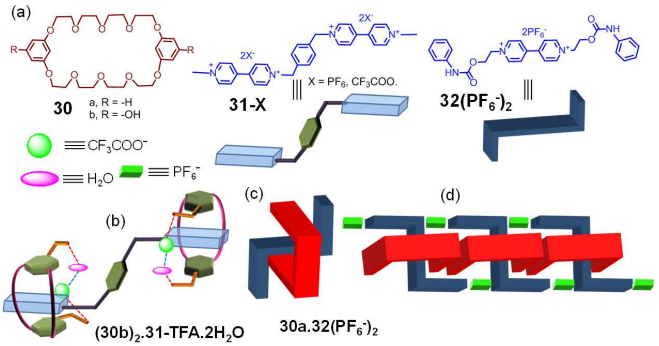

Figure 19. (a) Molecular structures for the host **30** and different guest molecules **31**, **32**; Schematic illustration of (b) a pseudocryptand based [3]pseudorotaxane formed between **30b** and **31**-TFA, (c) 1:1 complex of **30a** and **32**(PF$_6^-$)$_2$ and (d) a poly-pseudorotaxane where PF$_6^-$ acted as a bridge.

They also observed that in a supramolecular poly(taco complex) formation between **30a** and urethane derivative, **32**(PF$_6^-$)$_2$, PF$_6^-$ played a key role.[35] Each PF$_6^-$ counterion acted as a bridge through hydrogen bonding interactions to stabilize the non-covalent polymer (Figure 19d).

Huang and co-workers had utilized the preference of the urea functionality towards trifluro acetate and halide ions for demonstrating this phenomena and the associated photo-induced processes for adduct formation between divalent salts of paraquat with bis(m-phenylene)-32-crown-10 (**33**).[36] In the solid state, a pseudorotaxane structure was observed for CF$_3$COO$^-$ as counteranions of paraquat; however, "taco" complex formation prevailed when PF$_6^-$ or Cl$^-$ was used as counterions (Figure 20). The significant difference in conformation was achieved mainly due to the different packing geometry of the counter anion. Chloride ion was found to coordinate to two urea groups with a distorted tetrahedral geometry as well as the more efficient N-H…Cl$^-$ interaction contributed favourably in forming the poly(taco complex). These examples basically demonstrate the possibility of using appropriate counter anion for generating interesting selfassembled structures which otherwise are difficult to achieve and can be utilized as a design strategy.

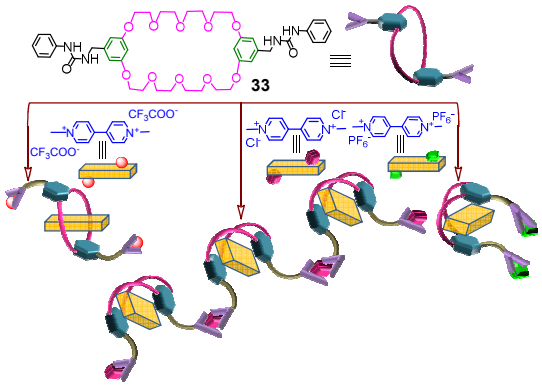

Figure 20. Cartoon representation of different mode complexation of macrocyclic host **33** with paraquat salt with different counter anion.

3.3 Conformational motion in cucurbit-uril based pseudorotaxane

Kim et al. first demonstrated that host-induced conformational change due to unusual back-folding of the guest containing both donor and acceptor moieties that led to the formation of an intramolecular charge transfer complex.[37]

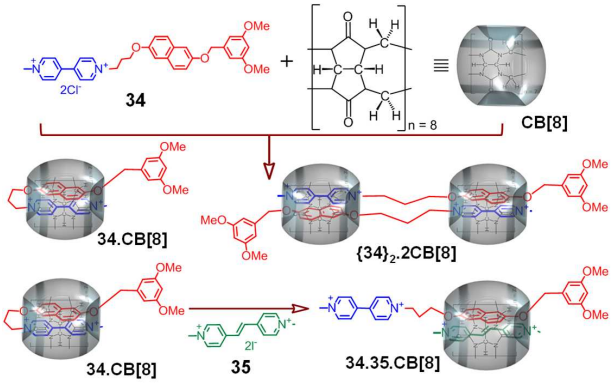

Figure 21. The structure of **34** and its probable conformational change in 1:1 complex **34**•CB[8] and intermolecular 1:1 complex (**34**)$_2$•2CB[8], and also the structure of the ternary complex **34**•**35**•CB[8] in presence of another guest **35**.

On addition of one mole equivalent of CB[8] to the aqueous solution of guest **34**, the solution turned violet due to the formation of a CT complex between napthyl moiety as donor and PQT^{2+} moiety as acceptor (Figure 21). Intramolecular CT complex formation adopted on formation of the folded conformation was confirmed from the results of the detailed ^{1}H-NMR spectral studies. Furthermore, it was also demonstrated that such intra-molecular CT interaction in

34•CB[8] could be disrupted by addition of competing donor or acceptor moiety and that resulted in a large conformation change. On addition of N,N′-dimethyldipyridyliumylethylene diiodide **35**, which was more electron deficient than a dialkyl-4,4'-bipyridinium unit, resulted in complete conversion of **34**•CB[8] to a ternary complex **34**•**35**•CB[8] by replacing the PQT^{2+} unit with **35**. Such ternary complex formation was confirmed by ^{1}H-NMR spectroscopy. Most importantly, this demonstrated that the guest in the supramolecular system **34**•**35**•CB[8] changed its conformation from a folded form to an extended form with associated changes in the CT spectra in response to an external chemical stimulus.

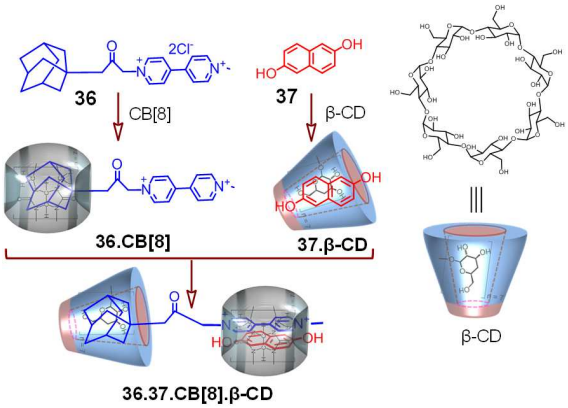

Figure 22. Molecular structure of **36** and its ternary complex formed with **37** in presence of β-CD and CB[8].

Recently, Liu et al. nicely demonstrated the concept of bottom-up approach for the formation of a quaternary complex as a result of guest exchange during complexation (Figure 22).[38] They reported a hetero-wheel [4]-pseudorotaxane **36**•**37**•CB[8] •β-CD. Thermodynamic driving force for this self-assembly formation was achieved by utilizing the simultaneous recognition of adamantyl moiety of **36** by β-CD and the CT interaction between **37** and viologen moiety of **36**, being included in the cavity of CB[8].

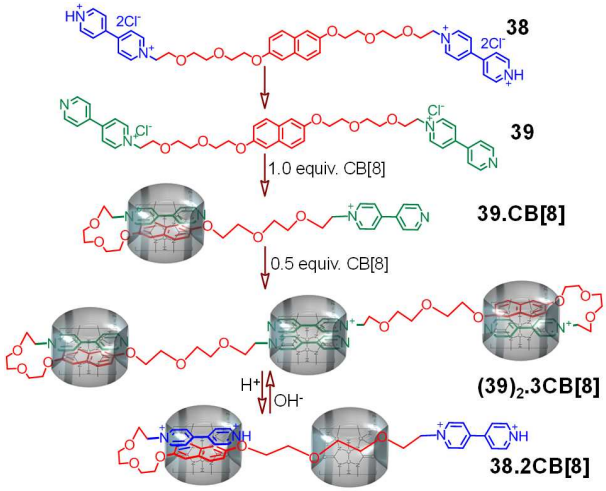

Figure 23. The structure of **39** and its probable conformational change in complexes **39**.CB[8] and (**39**)$_2$.3CB[8] and also acid/base driven control reversible complexation between (**39**)$_2$.3CB[8] and **38**.2CB[8].

The same group had nicely utilized the ability of the CB[8] to act as an efficient host for the folded CT complex formed between the napthyl and viologen moieties to demonstrate a supramolecular system which showed reversibility between the two complex in the presence of external stimuli such as acid or base (Figure 23).[39] Initially, the linear molecule 39 formed a [5]pseudorotaxane (**39**)**2**•**3**CB[8] with CB[8] through "pasting" of two axle molecules, in which one viologen unit in 39, constituted hetero-guest pair with the naphthalene unit to form the host-induced intra-molecular CT complex (**39**•CB[8]). While the other viologen unit formed a homo-guest pair with one of the viologen units of the other **39** in (**39**)$_2$•3CB[8]). Furthermore, this [5]pseudorotaxane (**39**)$_2$•3CB[8] transformed to a [3]pseudorotaxane 38•2CB[8], through detaching the two axle molecules in the presence of H^+, and subsequently addition of base resulted in a reversible switch between two different pseudorotaxanes.

4. Imidazolium as binding motif

Imidazolium derivatives as a suitable guest for interwoven complex formation were demonstrated successfully with various macrocyclic ligands as host fragments.[40,41] In the 1,3-disubstituted imidazolium salts, the pK_a of H-atom substituted at the C_2 proton varies between 16 to 24, depending on the nature of the substituents on two imidazolium nitrogens. These acidic protons act as hydrogen- bond donor and participate in the formation of supramolecular complexes. In addition to this the other non-covalent interactions, which are generally involved in binding are the ion dipole interactions and the electron deficient nature of the imidazolium ring which act as a π-acceptor.

One of our recent studies revealed that depending upon the length of the covalent linker in two bis-imidazolium derivatives **41** and **42**, corresponding [3]pseudorotaxane adducts adopted different conformation or orientation with varying π–π/donor–acceptor interaction (Figure 24).[42] For the host molecule **40**, two bis-azacrown moieties were linked by luminescent naphthalendiimide functionality, which was known for its π-acceptor nature. Detailed ^{1}H-NMR studies revealed two distinct conformations for the imidazolium ring as well as for the naphthalene and naphthalene diimide ring on formation of a host-guest adduct. For guest molecule with smaller covalent linker **41**, imidazolium ring adopted a perpendicular orientation with respect to phenyl ring; while, the naphthyl ring was located away from the diimide moiety and accounted for a weak π-π interaction (Figure 24b). In case of **42**, the imidazolium ring adopted a parallel orientation and the naphthyl ring showed strong π-π interaction with the diimide moiety on complexation (Figure 24c). Results of the electronic and fluorescence spectral studies also suggested the formation of a ground state complex for both examples of [3]pseudorotaxanes. Comparison of the K_a values for the two

complexes **40•(41)$_2$** and **40•(42)$_2$**, also reflects the higher flexibility of the linker in **42**, as the favourable factor for aligning the donor in a more symmetric fashion for more effective π–π stacking.

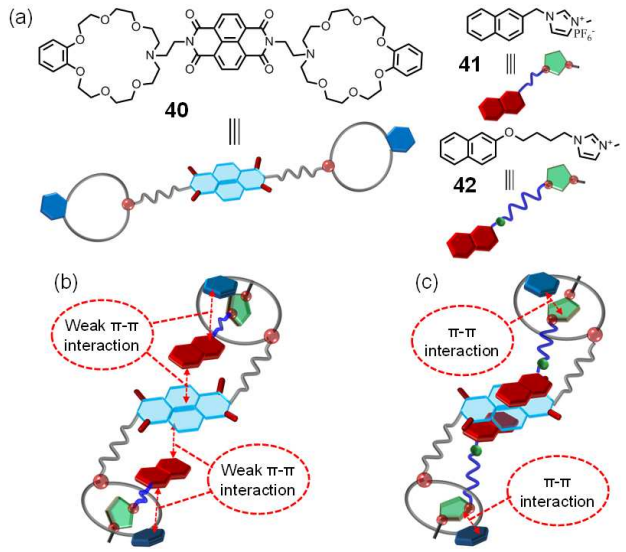

Figure 24. (a) The structure of the divalent host **40** and the two guest molecules **41** and **42**; (b) schematic presentation of the [3]pseudorotaxane **40•(41)$_2$** with perpendicular orientation of the imidazolium ring and the phenyl ring. (c) Schematic presentation of the [3]pseudorotaxane **40•(42)$_2$** with parallel orientation of the imidazolium ring and the phenyl ring.

We had also demonstrated the folding-unfolding movement of a crown ether moiety as host was induced by the pseudorotaxane formation while interacting with a guest having a pendant imidazolium ion (Figure 25a).[43] Computational studies revealed that the new DB24C8 derivative **19**, functionalized with aromatic moieties (naphthalene and coumarin), adopted a folded conformation (Figure 25b).

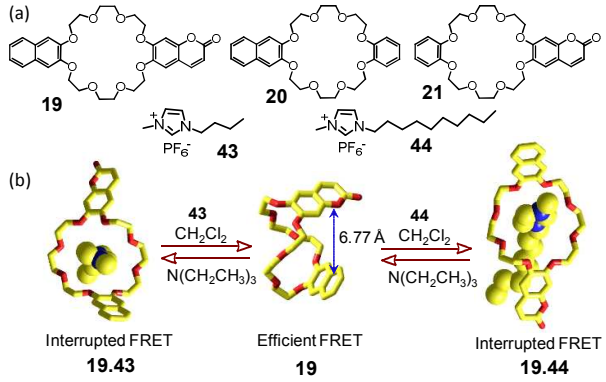

Figure 25. (a) Molecular structures of the hosts **19**, **20**, **21** and two guest molecules **43** and **44** and (b) energy optimized structures of host, **19** and the host-guest assemblies and their reversible complex formation with **43** and **44**. [Figure is reproduced from Ref 43]

This folded structure was stabilized by an efficient π–π stack interactions and such a conformational orientation was also suitable for an effective turn-ON FRET process between the donor naphthalene and acceptor coumarin moieties in **19**. However, on formation of [2]pseudorotaxane with imidazolium ion derivatives, **43** and **44**, the host ether **19** adopted an unfolded or open conformation (Figure 25b). The extent of unfolding process of the crown unit was found to depend on the alkyl chain length of the guest molecules. The increase in the effective distance between the naphthalene and coumarin moieties in the open conformation of pseudorotaxane was also evident in the decrease of the effective FRET-based luminescence response. Further this change in conformation, from the folded to an open one, was rationalized by computational as well as ^{1}H-NMR and X-ray single crystal studies. The reversible nature of this complexation process was also established in presence base or polar solvent like triethyl amine and DMSO (Figure 25b).

5. Miscellaneous photo-responsive assemble

Among many research groups, Huang and co-workers had made an extensive effort to utilize the process of pseudorotaxane formation for developing different microstructure as well as self-healing functional materials with photo-responsiveness in the assembled state.

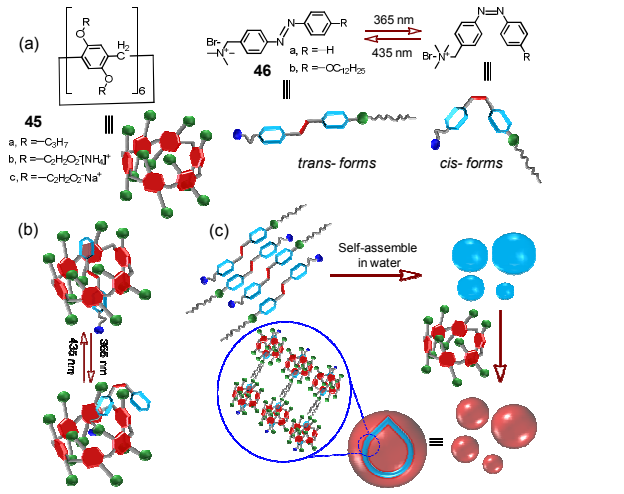

Figure 26. (a) Chemical structure of the pillararene based host molecule **45** and the guest molecules **46**; (b) Photo-induced complexation and decomplexation process of the host **45a** and guest **46a**; (c) Cartoon representation of the photo-responsive self-assembly between **45b** and **46b** in water.

For this, photo-responsive recognition motifs such as pillar[6]arene-based host **45** and the azobenzene containing guest **46** were used to demonstrate the self-assembly behaviour in organic solvents as well as in water (Figure 26).[44,45] Studies revealed that the cavity size of **45** was appropriate to accommodate the *trans*-form of the guest **46a**. This on excitation at 365 nm generated the corresponding *cis*-form and subsequently, the size mismatch led to a decomplexation process (Figure 26b). This reversible photo-controlled behaviour was used to fabricate different micro-structure in solution. Initially the *trans*-isomer of **46a** formed solid spherical aggregates of diameter ~92 nm, which disappeared on complexation with the host **45a**. Interestingly upon excitation at

365 nm, vesicle-like aggregates with average diameter of 5 μm were formed through self-assembly process of free *cis*-form produced through the decomplexation process. Use of amphiphilic guest molecules **46b** showed a distinct change in morphology from solid spherical nanoparticles to vascular like structure on complexation with host **45b** in water (Figure 26c). On photo excitation at 365 nm, spherical nanoparticles were formed through self-assembly of the dissociated *cis*-isomers.

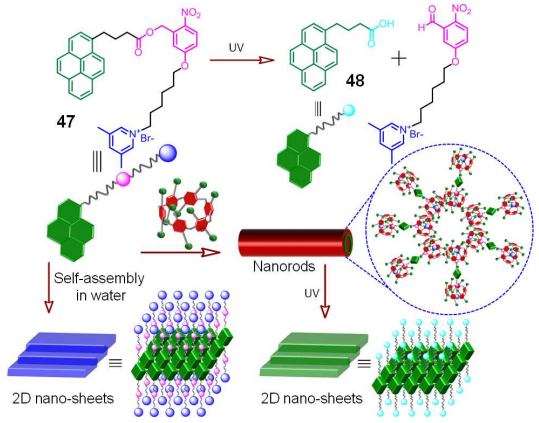

Figure 27. Chemical structure of supra-amphiphile **47** and the cartoon representation of photo-responsive self-assembly in water in presence of **45c**.

This research group had also designed a smart amphiphilic guest molecule **47**, where the hydrophilic and hydrophobic components were linked through a photo-cleavable 2-nitrobenzyl ester moiety (Figure 27).[46] This photo-cleavable property of this ester derivative was used to create well-defined and tuneable supramolecular architectures during the pseudorotaxane formation with the host **45c**. Initially **47** were found to self-assemble in water to form two-dimensional nano-sheets, which on complexation with **45c** converted to a nanorod. Photo-irradiation at 360 nm favoured the formation of the *cis*-isomer. This set off the dethreading process and led to generate two-dimensional nano-sheets through the favoured self-assembly process of pyrene-1-butyric acid **48** in water.

Huang and co-workers also reported smart adaptive materials by utilising the host-guest interaction of conjugated polymer with bis-ammonium salt as cross-linker.[47,48] These host-guest adducts showed interesting multiple stimuli dependent photo-response and self-healing property (Figure 28). Host DB24C8 units, covalently appended on a conjugated polymer **49** and the guest component **52** as the cross-linker were used for the fabrication of the smart of materials with different fluorescence responses in presence of different external stimuli. The conjugated polymer in its assembled state showed a weak fluorescence due to an efficient aggregation induced quenching process involving the main polymer chain. In presence of different stimuli such as potassium ion, chloride ion, pH increase, and heating the network structure was destroyed led to an enhancement in fluorescence. Exposure of a film of this cross-linked network to ammonia gas, also led to an increase in fluorescence. They have also used a PMMA-based polymer with pendent DB24C8 units **50**, to fabricate the cross-linking network with two bis-ammonium salts **51** and **52**. Cross-linking network obtained due to the inclusion complex formation between **50** and **52**, showed gel-sol and sol-gel transformation in presence of TEA and TFA, respectively. However, such reversibility was not observed for cross-linked adducts formed between **50** and **51**. Subtle structural difference in the thread, made the rethreading process slow. Thus, the small structural changes in the stopper units made one a pH stimuli dependent smart adaptive materials, whereas the other one a degradable material, although both showed interesting self-healing properties.

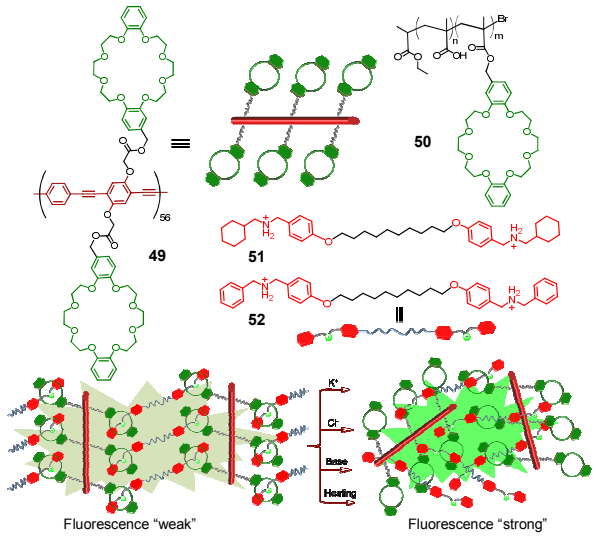

Figure 28. Chemical structure of conjugated polymers **49**, **50** and the two cross linker **51** and **52** along with the cartoon representation of the stimuli dependent assemble disassemble behaviour with different optical response.

5. Summary and Outlook

In this review article we have discussed the possibility of using optical responses for probing the changes in molecular conformation of the host and/or guest molecule(s) on formation of a pseudorotaxane or a taco-complex. We have tried to reveal the intricacies in designing such host and/or guest molecules and their appropriate functionalization with suitable fluorophores, which eventually would initiate a photo-induced process like PET, ICT transitions and FRET on change in their conformation(s). A close look at the database available for such assemblies, reveals that the thermodynamic stabilities are primarily achieved through certain non-bonding interaction like hydrogen bonding, π-π interaction as well as other electrostatic interactions like ion-dipole and dipole-dipole interaction. Such interactions contribute in adopting the eventual conformation of the assembly or the relative orientation of the individual host or guest component(s). Interestingly, π-π stacking interactions are operational over a distance that is also appropriate for the FRET based interactions. In this article we have also discussed, how this could be utilized in designing the appropriate host and/or guest molecules to achieve a new modified FRET based

fluorescence responses on change in conformation that adversely or favourably influence the FRET based interaction(s). There is/are certain prerequisite for other photo-induced processes like PET and CT transitions. We have talked about how such process(es) could be inherited while designing the host and/or guest molecules for the supramolecular assembly formation. We have also discussed how results of the fluorescence studies could be utilized in complementing results of the ^{1}H-NMR studies for predicting the relative change in orientation or conformation of the host and/or guest assembly(ies) in a supramolecular complex in solution state.

In brief, this review article has presented rational approaches that have been adopted by various research groups for designing some smart stimuli responsive functional supramolecular assemblies with interesting photo-physical property(ies). Such discussions are expected to contribute in developing a better insight in supramolecular chemistry, molecular recognition, mechanically interlocked molecule for the development of artificial molecular level machine, stimuli dependent self-assembly, molecular electronics (molecular logic operators) etc. Apart from these, discussion on optical responses as a function of the conformational changes is also expected to contribute in understanding complicated biological events that are generally associated with some conformational change(s).

Acknowledgements

A.D. thanks DST (India) and CSIR (India) for financial support. M. B. acknowledges CSIR for her research fellowship.

Notes and references

[a] University of Twente, Molecular Nanofabrication; Hallenweg 15, 7522 Enschede, The Netherland.

[b] Organic Chemistry Division, National Chemical Laboratory, Dr. Homi Bhabha Road, Pune, Maharashtra: 411008, India; Fax: +91(0)20 25902629; E-Mail: a.das@ncl.res.in.

1. F. Wang, C. Han, C. He, Q. Zhou, J. Zhang, C. Wang, N. Li and F. Huang, *J. Am. Chem. Soc.*, 2008, **130**, 11254-11255.
2. Z. Zhang, Y. Luo, J. Chen, S. Dong, Y. Yu, Z. Ma and F. Huang, *Angew. Chem. Int. Ed.*, 2011, **50**, 1397-1401.
3. X. Ji, S. Dong, P. Wei, D. Xia and F. Huang, *Adv. Mater.*, 2013, **25**, 5725-5729.
4. S. Dong, B. Zheng, F. Wang and F. Huang, *Acc. Chem. Res.*, 2014, **47**, 1982-1994.
5. X. Yan, D. Xu, X. Chi, J. Chen, S. Dong, X. Ding, Y. Yu and F. Huang, *Adv. Mater.*, 2012, **24**, 362-369.
6. S. Dong, B. Zheng, D. Xu, X. Yan, M. Zhang and F. Huang, *Adv. Mater.*, 2012, **24**, 3191-3195.
7. S. Dong, Y. Luo, X. Yan, B. Zheng, X. Ding, Y. Yu, Z. Ma, Q. Zhao and F. Huang, *Angew. Chem. Int. Ed.*, 2011, **50**, 1905-1909.
8. Z. Zhang, G. Yu, C. Han, J. Liu, X. Ding, Y. Yu and F. Huang, *Org. Lett.,* 2011, **13**, 4818-4821.
9. P. R. Ashton, I. Baxter, M. C. T. Fyfe, F. M. Raymo, N. Spencer, J. F. Stoddart, A. J. P. White and D. J. Williams, *J. Am. Chem. Soc.*, 1998, **120**, 2297-2307.
10. G. Yu, M. Xue, Z. Zhang, J. Li, C. Han and F. Huang, *J. Am. Chem. Soc.*, 2012, **134**, 13248-13251.
11. C. J. Pedersen, *J. Am. Chem. Soc.*, 1967, **89**, 7017-7036.
12. C. J. Pedersen, *Angew. Chem. Int. Ed.*, 1988, **27**, 1021-1027.
13. K. N. Trueblood, C. B. Knobler, D. S. Lawrence and R. V. Stevens, *J. Am. Chem. Soc.*, 1982, **104**, 1355-1362.
14. P. R. Ashton, P. J. Campbell, P. T. Glink, D. Philp, N. Spencer, J. F. Stoddart, E. J. T. Chrystal, S. Menzer, D. J. Williams and P. A. Tasker, *Angew. Chem. Int. Ed.*, 1995, **34**, 1865-1869.
15. P. R. Ashton, P. T. Glink, C. Schiavo, J. F. Stoddart, E. J. T. Chrystal, S. Menzer, D. J. Williams and P. A. Tasker, *Angew. Chem. Int. Ed.*, 1995, **34**, 1869-1871.
16. S. Shinkai, M. Ishihara, K. Ueda and O. Manabe, *J. Chem. Soc., Perkin Trans. 2*, 1985, 511-518.
17. A. K. Mandal, M. Suresh, P. Das and A. Das, *Chem. Eur. J.*, 2012, **18**, 3906-3917.
18. M. Montalti, R. Ballardini, L. Prodi and V. Balzani, *Chem. Commun.*, 1996, 2011-2012.
19. E. Ishow, A. Credi, V. Balzani, F. Spadola and L. Mandolini, *Chem. Eur. J.*, 1999, **5**, 984-989.
20. A. K. Mandal, M. Suresh, M. K. Kesharwani, M. Gangopadhyay, M. Agrawal, V. P. Boricha, B. Ganguly and A. Das, *J. Org. Chem.*, 2013, **78**, 9004-9012.
21. Y.-M. Zhang, M. Han, H.-Z. Chen, Y. Zhang and Y. Liu, *Org. Lett.*, 2013, **15**, 124-127.
22. M. Han, H.-Y. Zhang, L.-X. Yang, Q. Jiang and Y. Liu, *Org. Lett.*, 2008, **10**, 5557-5560.
23. Z.-J. Ding, Y.-M. Zhang, X. Teng and Y. Liu, *J. Org. Chem.*, 2011, **76**, 1910-1913.
24. H.-B. Cheng, H.-Y. Zhang and Y. Liu, *J. Am. Chem. Soc.*, 2013, **135**, 10190-10193.
25. M. Suresh, A. K. Mandal, E. Suresh and A. Das, *Chem. Sci.*, 2013, **4**, 2380-2386.
26. Y. Zeng, Y. Li, M. Li, G. Yang and Y. Li, *J. Am. Chem. Soc.*, 2009, **131**, 9100-9106.
27. M. Zhang, K. Zhu and F. Huang, *Chem. Commun.*, 2010, **46**, 8131-8141.
28. B. Zheng, F. Wang, S. Dong and F. Huang, *Chem. Soc. Rev.*, 2012, **41**, 1621-1636.
29. F. Wang, J. Zhang, X. Ding, S. Dong, M. Liu, B. Zheng, S. Li, L. Wu, Y. Yu, H. W. Gibson and F. Huang, *Angew. Chem. Int. Ed.*, 2010, **49**, 1090-1094.
30. G. Yu, X. Zhou, Z. Zhang, C. Han, Z. Mao, C. Gao and F. Huang, *J. Am. Chem. Soc.*, 2012, **134**, 19489-19497.
31. X. Yan, F. Wang, B. Zheng and F. Huang, *Chem. Soc. Rev.*, 2012, **41**, 6042-6065.
32. A. K. Mandal, P. Das, P. Mahato, S. Acharya and A. Das, *J. Org. Chem.*, 2012, **77**, 6789-6800.
33. J. W. Jones, L. N. Zakharov, A. L. Rheingold and H. W. Gibson, *J. Am. Chem. Soc.*, 2002, **124**, 13378-13379.
34. F. Huang, I. A. Guzei, J. W. Jones and H. W. Gibson, *Chem. Commun.*, 2005, 1693-1695.
35. F. Huang, F. R. Fronczek and H. W. Gibson, *Chem. Commun.*, 2003, 1480-1481.
36. K. Zhu, S. Li, F. Wang and F. Huang, *J. Org. Chem.*, 2009, **74**, 1322-1328.

37. J. W. Lee, K. Kim, S. Choi, Y. H. Ko, S. Sakamoto, K. Yamaguchi and K. Kim, *Chem. Commun.*, 2002, 2692-2693.
38. Z.-J. Ding, H.-Y. Zhang, L.-H. Wang, F. Ding and Y. Liu, *Org. Lett.*, 2011, **13**, 856-859.
39. Z.-J. Zhang, H.-Y. Zhang, L. Chen and Y. Liu, *J. Org. Chem.*, 2011, **76**, 8270-8276.
40. S. Dong, B. Zheng, Y. Yao, C. Han, J. Yuan, M. Antonietti and F. Huang, *Adv. Mater.*, 2013, **25**, 6864-6867.
41. S. Dong, J. Yuan and F. Huang, *Chem. Sci.*, 2014, **5**, 247-252.
42. A. K. Mandal, M. Suresh and A. Das, *Org. Biomol. Chem.*, 2011, **9**, 4811-4817.
43. M. Suresh, A. K. Mandal, M. K. Kesharwani, N. N. Adarsh, B. Ganguly, R. K. Kanaparthi, A. Samanta and A. Das, *J. Org. Chem.*, 2010, **76**, 138-144.
44. G. Yu, C. Han, Z. Zhang, J. Chen, X. Yan, B. Zheng, S. Liu and F. Huang, *J. Am. Chem. Soc.*, 2012, **134**, 8711-8717.
45. D. Xia, G. Yu, J. Li and F. Huang, *Chem. Commun.*, 2014, **50**, 3606-3608.
46. J. Yang, G. Yu, D. Xia and F. Huang, *Chem. Commun.*, 2014, **50**, 3993-3995.
47. M. Zhang, D. Xu, X. Yan, J. Chen, S. Dong, B. Zheng and F. Huang, *Angew. Chem. Int. Ed.*, 2012, **51**, 7011-7015.
48. X. Ji, Y. Yao, J. Li, X. Yan and F. Huang, *J. Am. Chem. Soc.*, 2012, **135**, 74-77.

